Turbulent secondary atomization of non-evaporating dilute spray jets

A. Kourmatzis* and A. R. Masri
Aerospace, Mechanical and Mechatronic Engineering, The University of Sydney, NSW 2006, Australia
akourmatzis@sydney.edu.au and assaad.masri@sydney.edu.au

Abstract

The secondary atomization characteristics of dilute spray jets of mineral turpentine with varying levels of turbulence are investigated using phase Doppler anemometry (PDA). The choice of mineral turpentine as the injected liquid ensures no evaporation at room temperature and a dilute spray is utilized to avoid droplet-droplet interactions. The spray is formed upstream of a pipe and is carried with air to the jet exit plane. The influence of turbulence on secondary atomization is studied in this paper via presentation of the Sauter mean diameter (SMD), droplet diameter probability density functions (PDFs), and scatter plots of the droplet Weber (We_d) vs. Ohnesorge (Oh_d) number. A range of Reynolds numbers from ∼12,000-37,000 are tested with tube lengths varying from 4.7 to 43 jet diameters. The focus is on data from measurements taken at the tube exit planes where the effects of dispersion are minimal. All of the aforementioned simplifications allow for the authors to attribute changes in droplet diameter predominantly to secondary atomization. Scatter plots of the droplet We_d vs. Oh_d reveal that in the investigated geometry, $We_d << 10$ for $Oh_d < 0.1$ due to the low droplet slip velocity, indicating that only droplet deformation would be occuring in an analogous non-turbulent gas flow. However, it is found that the SMD decreases by as much as $20\mu m$ with increasing Reynolds number and by $10\mu m$ with increasing tube length. Increasing the tube length from 4.7 to 43 diameters whilst keeping the Reynolds number constant results in a different flow profile at the exit plane, varying from under-developed, to transitional, and finally to a fully developed turbulent flow. This increase in tube length leads to a consistent decrease in the SMD of the dilute spray, acting as evidence of turbulence enhanced secondary atomization.

Keywords: secondary atomization, turbulent atomization, dilute spray, PDA

Introduction

Spray formation in applications with or without heat release is a complex process that nominally occurs in stages referred to as primary and secondary atomization followed by a region where droplets become more dispersed in the gas phase [1, 2]. The focus of this paper is on secondary atomization where a drop moving at a relative velocity to the surrounding gas phase further fragments into smaller droplets. In spray combustion, small droplet sizes are a neccesity if rapid evaporation and subsequent ignition is to occur. The study of droplet break-up is therefore vital in order to assist with the design of atomization systems that can promote efficient secondary atomization and therefore increase combustion efficiency. Conventional secondary atomization of a droplet has been studied to some detail and occurs when a droplet is moving at a high velocity relative to the surrounding gas phase. Some of the most fundamental work in characterising the nature of secondary atomization has been reviewed extensively by Faeth and co-workers [3, 4] and more recently by Guildenbecher et al. [1]. Investigation of the nature of secondary atomization is done using methods such as continuous jet [5, 6] and shock tube methods [7, 8] and recently, novel fuels such as biofuels [9] have been tested. A number of different droplet break-up regimes may be delineated as functions of the droplet Weber number (We_d) and Ohnesorge number (Oh_d) defined in Eq. 1 where ρ_g is the gas-phase density, U is the droplet velocity, U_g is the gas phase velocity, D is the droplet diameter, σ the surface tension and μ_l the droplet viscosity.

$$We_d = \frac{\rho_g (U - U_g)^2 D}{\sigma_l} \qquad Oh_d = \frac{\mu_l}{\sqrt{\rho_l \sigma D}} \tag{1}$$

Different break-up regimes include ‘bag break-up’, ‘multi-modal break-up’ and ‘shear break-up’ [3, 8] which, for an $Oh_d < 0.1$ occur at $We_d > 11$, $We_d > 35$ and $We_d > 80$ respectively. The physics of aerodynamic secondary atomization has been further investigated by numerous researchers fully reviewed in the recent review paper by Guildenbecher et al. [1]. Models for secondary atomization have been proposed by Wu et al. [10]

*Corresponding author: akourmatzis@sydney.edu.au

which give an estimate of the Sauter mean diameter (SMD) of the 'children' droplets resulting from a secondary atomization event. These empirical models did yield some success even when using a range of different liquid properties and comparing to available experimental data [3].

One subject that has yet to receive significant attention is the secondary atomization of droplets in a turbulent flow, even though single droplet studies of turbulence enhanced evaporation for example have been reported in detail [11]. The original work of Kolmogorov [12] and Hinze [7] suggested that any droplets larger than the smallest turbulent length-scale may undergo turbulent atomization as a result of velocity fluctuations. This was examined to some degree by Sevik and Park [13] who defined a critical Weber number of 1.3 which could also be theoretically defined by analysing the droplet 'resonances' of a turbulent flow. The same critical Weber number was applied to bubble break-up in a high Reynolds number water jet. As also reviewed by Guildenbecher et al. [1] turbulence will 'add randomness to the break-up process' thereby possibly leading to a host of different break-up regimes that depart from the conventional bag break-up and multi-modal break-up modes. Further experimental work was carried out by Lasheras et al. [14] on the primary and secondary atomization of droplets issued from a high speed annular jet and the authors carried out a rigorous study using high speed visualisation and phase Doppler anemometry (PDA) to describe the turbulent break-up phenomena. A main finding was that the total kinetic energy supplied by the gas phase was a key quantity in determining the secondary atomization far from the liquid core.

Though a handful of investigations have been carried out, turbulent secondary atomization has not received much attention in the literature. This paper presents a systematic study investigating secondary atomization in a dilute turbulent droplet laden jet by varying the Reynolds number and level of turbulence development within a pipe. These two key quantities are varied by altering the air jet velocity and tube length respectively. Varying the tube length from 'short' to 'long' changes the flow from under-developed to fully developed turbulent flow respectively, and the droplet sizes are examined at the exit plane of these tubes for a fixed fuel to air ratio using PDA. The use of a simple yet well-defined geometry allows for generalisation of the results and may provide modellers with useful information regarding the evolution of droplet size in elevated Reynolds number droplet laden jets. The paper begins by outlining the experimental set-up utilized, and then proceeds to characterising the flows via investigation of velocity profiles and SMD profiles across the jet. PDFs of droplet size are then used to quantify the effect of turbulence on the droplet size and this is then followed by scatter plots of the droplet We_d vs. Oh_d numbers. The paper concludes by commenting on the Kolmogorov length scales associated with these flows with respect to the change in droplet size with increasing turbulence.

Experimental Methods

The dilute mineral turpentine spray is generated using a Sonotek ultrasonic nebulizer that is rated to produce an SMD of 40 μm when used with water. The density ρ_l of mineral turpentine is taken as 810 kg/m^3, the dynamic viscosity μ_l as 0.00137 Pas and the surface tension σ_l as 0.0225 N/m. The generated spray is convected downstream through the main fuel tube of length L, which takes values of 22mm (short tube), 101mm (mid-length tube) and 196mm (long tube) respectively and has a fixed diameter d of 4.6mm as may be seen in Fig. 1. The distance from the nebulizer tip and fuel tube entry point was chosen based on previous experiments [15]. The previous experiments have shown this particular geometry to be an optimal configuration in terms of generating a uniform dilute spray at the exit plane with minimal droplet impaction at the fuel entry point into the tube. Five cases shall be presented in this paper named cases 'A2' to 'A6' which are fully described in Table 1. The carrier air and liquid fuel flow-rates are measured using flow-meters with an accuracy of approximately 1% and 5% respectively.

A commercial PDA system (TSI Model FSA 3500/4000) was utilized for the measurements. The detector, with a 300-mm focal length and 3.2 μm fringe spacing, was positioned at 45 degrees in the forward scattering mode. An Argon-ion laser feeds the dual channel fiber optics assembly which trasmits a beam pair with wavelengths of 514.5 nm and 488 nm which are used for measuring the axial and radial components of velocity respectively. A Bragg cell shifts one beam from each pair by 40 MHz to allow for differentiation between measurement of velocity in the 'positive' and 'negative' directions. Typical sampling rates were above 10kHz at the spray centreline but could be as low as 500Hz at the spray periphery, and 10,000 samples were typically collected at each measurement location with velocity validation of 90% and above being common for both axial and radial measurement channels. Discussion of the current PDA system has been reported elsewhere [15].

Results and Discussion

Exit plane and downstream profiles

Measurements of axial mean velocity and SMD (also referred to herein as D32) are presented as a function of radial position across the jet for various downstream positions (x/D) for case A5 in Figs. $2(a)$ to $2(d)$. These

Case	U_j m/s	Re_j	M_f g/min	M_g g/min
A2	40	12266	9.6	47.8
A3	60	18400	14.4	71.8
A4	80	24533	19.1	95.7
A5	100	30667	23.9	119.6
A6	120	36800	28.7	143.5

Table 1. Test conditions for cases A2 to A6 for a constant fuel to air ratio equal to 0.2

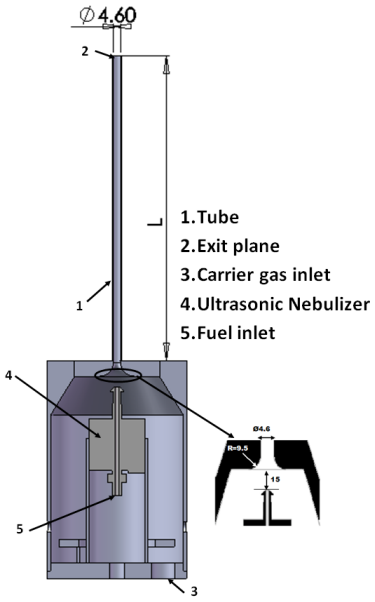

Figure 1. *Schematic of dilute spray generation set-up*

measurements are shown both for the short and long tubes in order to note features of interest.

The long tube yields a fully developed turbulent flow as may be seen through Fig. $2(a)$, and a point to note for this case is the drop in SMD at the spray centreline shown in Fig. $2(b)$. This is clearly predominant at x/D=0 and x/D=5, however dissipates further downstream due to dispersion. We assume that the significantly lower D32 at the centreline is present due to secondary atomization occuring prior to the liquid's exit from the tube, which creates a smaller droplet population in the centre. Given that the nebulizer is centred within the tube, it is logical to assume that the larger droplets that are less likely to migrate towards the tube wall remain in the centre of the tube and therefore break-up in the centre. The short tube does not exhibit this characteristic profile as may be seen in Fig. $2(d)$, and neither does the mid-length tube (not shown here for brevity), showing that it is only when the turbulence becomes fully developed that this change in droplet D32 profile occurs. One of the aims of this paper is to determine the cause of this droplet size reduction, as it is known that these droplet laden jets are turbulent and therefore any break-up should be turbulence assisted. The reader should further note that this drop in D32 at the spray centreline does not occur for lower Reynolds number cases, particularly for cases A1-A4, showing that the profile is dependant on the Reynolds number.

Exit plane D32 profiles

We now further comment on the evolution of the droplet size at the exit plane amongst the various tube lengths by examining the full range of Reynolds numbers as may be seen through Figs. $3(a)$ to $3(c)$. For lower Reynolds numbers, the change in droplet size when moving from one tube length to the other is less significant and this is

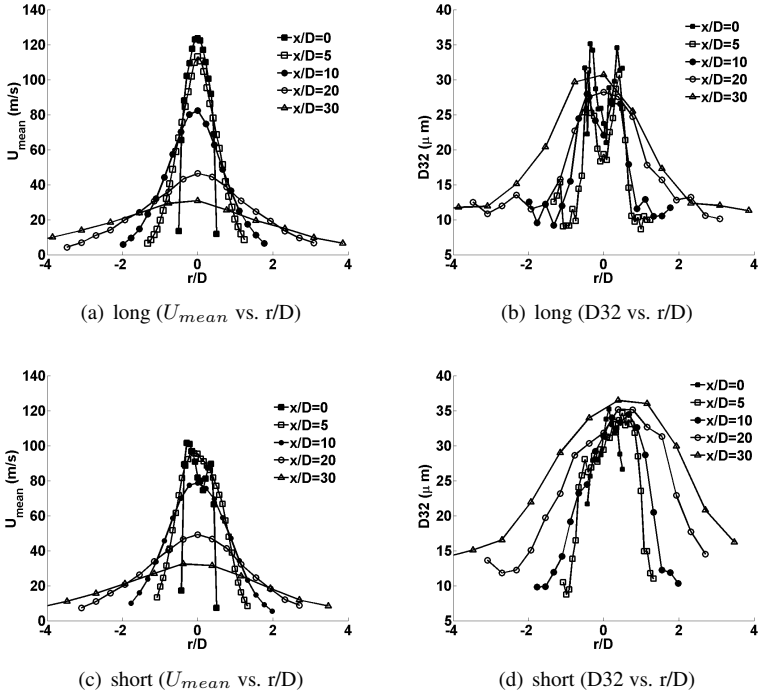

(a) long (U_{mean} vs. r/D) (b) long (D32 vs. r/D)

(c) short (U_{mean} vs. r/D) (d) short (D32 vs. r/D)

Figure 2. D32 and U_{mean} vs. r/D for case A5 as a function of downstream position for the long and short tubes

made clearer through Fig. 4 which shows the evolution of the centreline D32 values as a function of tube length and Reynolds number.

In the low Reynolds number case the droplets break-up by only a slight amount when going from one length to the next, due to both the low slip velocities and the low level of turbulence. Examining case A2 for example, the D32 drops slightly from 43 μm to 42 μm at the centreline from the short to the mid tube and then drops to around 39 μm at the long tube. Taking one of the higher Reynolds number cases, such as A6, the drop in D32 is 28 μm-19 μm when going from the short to the long tube.

In all of the cases a more significant drop in size is observed from the mid-length tube to the full length-tube. This shows that break-up cannot solely be occuring by conventional secondary atomization modes. If for example a bag-breakup regime was the dominant break-up mode in this spray, then most of the atomization would occur in areas of high slip velocity, e.g. when going from the short to the mid-length tube. If that were the case small droplet sizes would be measured at the short tube exit plane which would subsequently remain constant when moving from the mid to the long tube lengths.

It may be that many of the droplets break up at the entry of the spray into the tube (zoomed in region of Fig. 1) and that the reduction in size that is observed is solely due to the time taken for the droplets to break-up as they traverse the tube length. However, calculating the droplet break-up length as $l_b = (5D(\rho_l/\rho_g)^{1/2})$ [3] (assuming the droplets are convected only by U_0) suggests that the droplets cannot only be atomizing at the entry of the tube where the slip velocity is highest. Taking for example D to be equal to $50\mu m$, $30\mu m$ and $20\mu m$, the break-up distances l_b are equal to 6.5mm, 5.2mm and 3.9mm respectively, which are 1.4, 1.1 and 0.8 tube diameters respectively. The calculation suggests that if the droplets were breaking up from a conventional secondary atomization mode, their size would not decrease any further past a length equal to the short tube length.

Diameter distributions

While the D32 radial profiles show changes in droplet size, observation of the diameter distributions will give us insightful information regarding how the level of turbulence development in the tube affects the droplet size distribution at a given location. In order to examine this closely, PDFs of droplet size were produced for cases A2-A6 for the short, mid-length and long tubes as may be seen through Figs. $5(a)$ to $5(f)$. It is clear from case A2 (Figs. $5(a)$ and $5(b)$), that there is minimal change in the droplet size PDF amongst the various tube lengths, showing clearly, as with the D32 results that there is minimal atomization for case A2. For cases A4-A6 however there is a significantly higher population of $10\mu m$ droplets for the longer tube when compared to the shorter

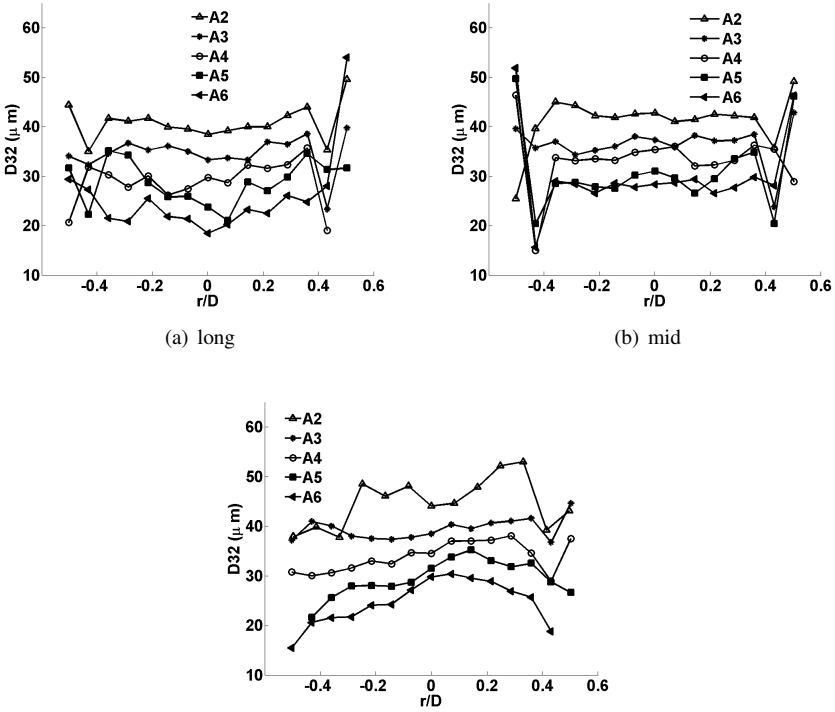

(a) long (b) mid

(c) short

Figure 3. D32 vs. r/D for all Reynolds numbers as a function of tube length at x/D=0

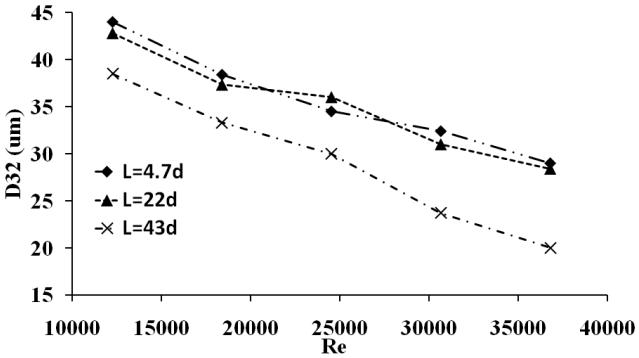

Figure 4. *D32 at spray centreline as a function of Reynolds number for the short, mid-length, and long tubes all at x/D=0*

variants. It is also clear that there is a downward shift in the probability of larger droplet sizes with increasing tube length, which is particularly evident in Figs. $5(e)$ and $5(f)$, showing that the larger droplets are atomizing and are being binned in the $5 - 15\mu m$ range. While it was previously thought that there was minimal atomization in such dilute sprays it is now clear that for a sufficiently high Reynolds number this is not the case, at least prior to ejection from the exit plane.

Weber number scatter plots

The hypothesis that turbulence is enhancing the level of secondary atomization is further investigated by examining conventional droplet Weber numbers. In Figs. $6(a)$ to $6(f)$ the droplet Weber number has been calculated based on a given droplet's instantaneous velocity and a mean gas phase velocity. Ideally, a gas phase velocity associated with the surroundings of each individual droplet would be utilized, however as this is not possible to extract from the measurements we assume that the mean gas phase velocity represents the gas phase surrounding every droplet, and may be accurately represented by the mean velocity of the smallest droplets in the flow, namely

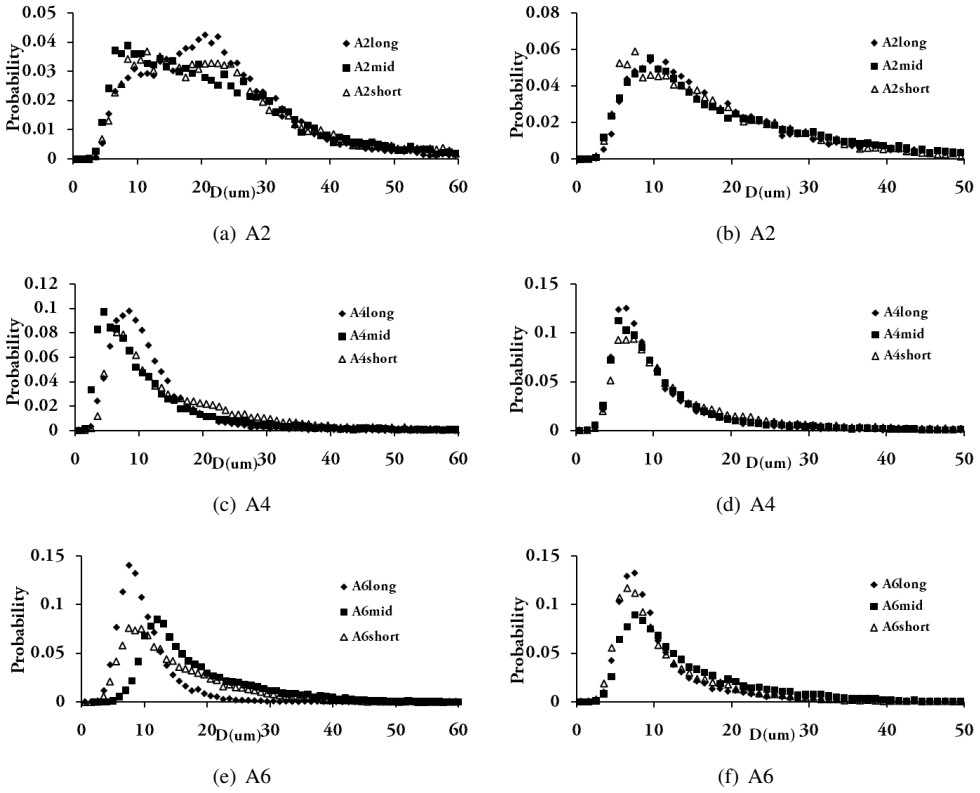

(a) A2 (b) A2

(c) A4 (d) A4

(e) A6 (f) A6

Figure 5. PDFs of droplet diameter at spray centreline (left) and at r/D=0.4 (right) at x/D=0 for all Reynolds number cases as a function of tube length

those from a size of $0 - 10\mu m$

If conventional atomization were occuring, then a Weber number of approximately $We_d > 11$ would indicate a bag-breakup regime with larger Weber numbers indicating multi-modal break-up and shear break-up regimes [8]. The theoretical bottom limit where conventional secondary atomization would commence is shown with a horizontal line on figure $6(a)$, where region 'A' indicates conventional secondary atomization which is not turbulence assisted and 'B' indicates the conventional deformation region. While the axial velocities are generally high in this geometry, the measurements taken at the exit plane are taken from droplets that already have sufficient axial momentum and therefore the slip velocities and force of acceleration on the droplets is low. The Weber number must be defined by the slip velocity given that conventional break-up regimes have been determined by experiments that issue a droplet of zero axial momentum into a high speed cross-flowing air jet or into a shock tube. The highest slip velocities are present in the short tube, where large droplets have not yet accelerated, and this is especially true for case A6. Indeed, it may be seen that the scatter plot of the droplet Weber number for the short tube of case A6, shown in Fig. $6(f)$ does reach a value close to 12, however the vast majority of droplets are theoretically not atomizing according to this analysis.

Furthermore, going from the short to the long tube for any of the Reynolds number cases generally yields a decrease in droplet Weber number, however this has coincided with a decrease in droplet size (see Fig. 4), confirming that it is not a conventional droplet atomization regime which is resulting in secondary atomization. The Weber numbers of the droplets while not enough to create shear break-up are enough to create deformation, particularly for the higher Reynolds number cases where oscillatory deformation may occur. The data shown suggests that turbulence is causing the secondary atomization observed in the spray, and the impact of the turbulence may be enhanced due to the fact that the flow is acting on deformed droplets.

Droplet size and Kolmogorov length

For droplets to be able to atomize through the action of turbulent fluctuation they must be greater than the Kolmogorov length [12, 13]. It is not immediately obvious whether or not this is the case, given that higher Reynolds numbers result in both an increase in the rms fluctuating velocity which will define the smallest length-

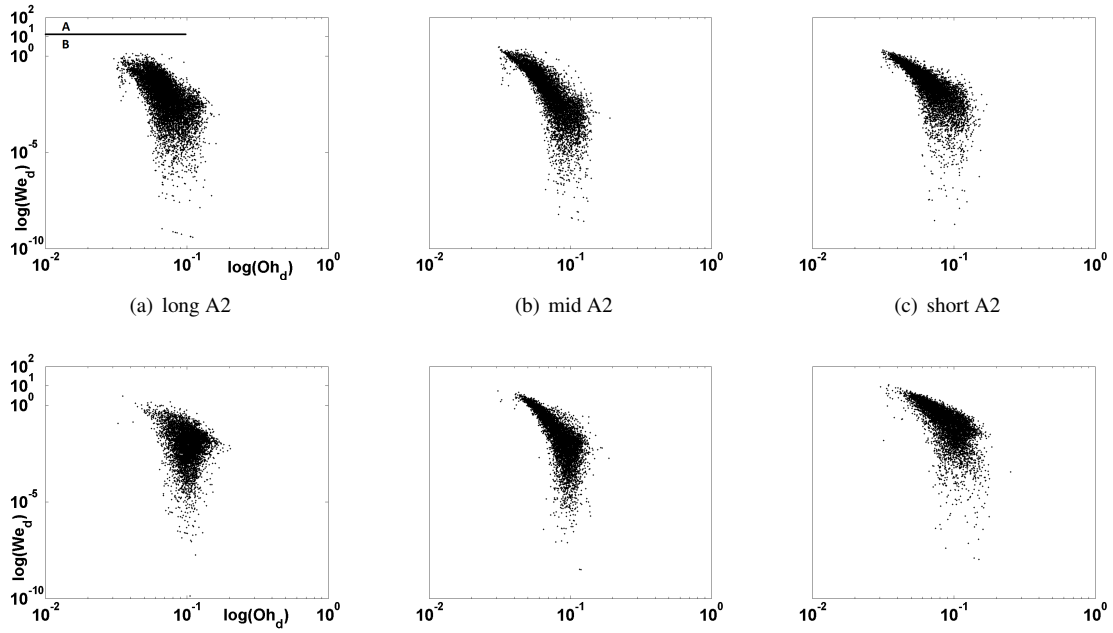

(a) long A2 (b) mid A2 (c) short A2

(d) long A6 (e) mid A6 (f) short A6

Figure 6. Log-log scatter plots of Weber number vs. Ohnesorge number for cases A2 and A6 at spray centreline at x/D=0 for all tube lengths where region 'A' corresponds to conventional secondary atomization, and region 'B' corresponds to conventional droplet deformation regimes

scale in the flow, while a higher velocity and thus Reynolds number is also what results in the reduction in droplet size. However, assuming that the droplets are breaking up due to the turbulent fluctuations, then by definition, they must always be greater than the Kolmogorov length. This analysis will provide insight regarding the deviation of a droplet size from the Kolmogorov length as a function of radial position and Reynolds number.

The Kolmogorov length is calculated as $\eta = (\nu_g^3/\epsilon)^{1/4}$ where $\epsilon = u_g'^3/\Lambda$ and u_g' is the rms axial velocity of the gas phase. Λ is the integral length-scale, estimated as $\Lambda = 0.65R_h$ where the half-radius $R_h = 0.0845X_L$ [16] and X_L is the axial location downstream equal to 0.3. Figure $7(a)$ shows the Sauter mean diameter vs. r/D for various Reynolds numbers all conditioned on the $0 - 10\mu m$ droplet range. The trend of $D32/\eta$ generally follows the trend of the axial rms velocity, given the relationship we have used between the Kolmogorov length and u', and these trends are similar to profiles that may be found in Chen et al. [17] or Starner et al. [18] . Clearly at the 0-10 μm range none of the cases from A2-A5 are able to atomize at the spray centreline under the influence of turbulent fluctuations, but theoretically case A6 may be prone to turbulence enhanced atomization. However, even for case A6, across the full radial profile, the droplet sizes are only 1.5-2 times greater than the Kolmogorov length, indicating that it is generally unlikely that any droplets from $0 - 10\mu m$ would atomize, as is expected intuitively. In the 20-30 μm range of Fig. $7(b)$ it may be seen that the D32 is now at least twice the Kolmogorov scale in the centre of the spray and can increase to as high as one order of magnitude larger in the shear layer.

The results suggest that droplets located at r/D=0.4 would be more prone to break-up due to turbulence, however through our measurements it is difficult to substantiate this claim given that at r/D=0.4, droplets measured may also be those that have migrated from the centre due to some inevitable dispersion. Nevertheless, the results do show a consistent decrease in droplet size when moving from the shorter to longer tube lengths and this is more severe for higher Reynolds numbers. Imaging of these sprays using high magnification lens would provide further information regarding the physics of the turbulent atomization in these systems.

Summary and Conclusions

Secondary atomization has been observed in dilute spray jets of mineral turpentine. The break-up has been attributed to the varying degree of turbulence that has been applied by varying the jet velocity and tube length. The SMD decreases by up to 20 μm with increasing Reynolds number and by up to $10\mu m$ with increasing tube length. It has been determined that the droplet Weber numbers of the droplets are not sufficient enough for conventional break-up to occur, supporting the argument of turbulence enhanced secondary atomization made by the authors.

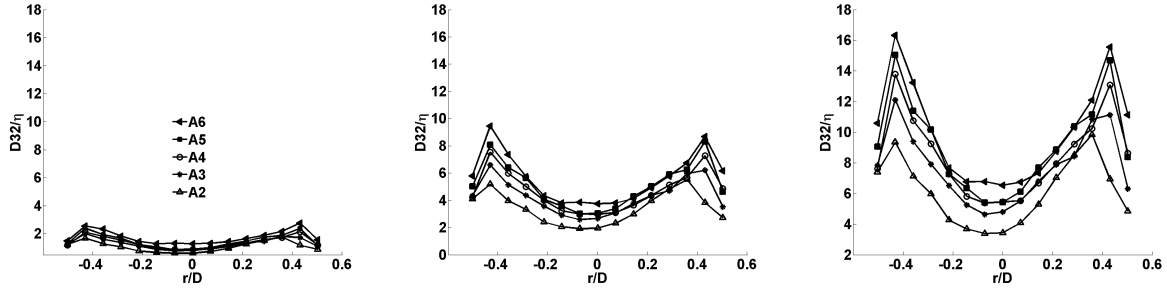

(a) $0 - 10\mu m$ (b) $20 - 30\mu m$ (c) $40 - 50\mu m$

Figure 7. Conditional D32 normalized by Kolmogorov length η vs. r/D as a function of Reynolds number for the mid-length tube

The D32 profiles of the various jets have been normalized by the Kolmogorov length across the jet profile showing that the D32/η varies anywhere from 2 to 16 depending on the radial location. The droplets located at r/D=0.4 are theoretically more prone to atomization by turbulence. Further work using imaging methods should be carried out in order to fully understand the atomization modes in the system.

Acknowledgements

The authors acknowledge William O'Loughlin and Dr. Vinayaka Prasad for insightful comments. The spray apparatus was designed by William O'Loughlin. The work is supported by the Australian Research Council.

References

[1] Guildenbecher, D.R. , López-Rivera, C. and Sojka, P.E. *Experiments in Fluids* 46,371-402 (2009)
[2] Dumouchel, C. *Experiments in Fluids* 45,371-422 (2008)
[3] Faeth, G.M., Hsiang, L.P. and Wu, P.K. *International Journal of Multiphase Flow* 21,99-127 (1995)
[4] Hsiang, L.P. and Faeth, G.M. *International Journal of Multiphase Flow* 18, 635-652 (1992)
[5] Liu Z. and Reitz, R.D. *International Journal of Multiphase Flow* 23, 631-650 (1997)
[6] Arcoumanis, C., Whitelaw, D.S. and Whitelaw, J.H *Atomization and Sprays* 6, 245-256 (1996)
[7] Hinze, J.O. *American Institute of Chemical Engineering* 1, 289-295 (1955)
[8] Hsiang, L.P. and Faeth, G.M. *International Journal of Multiphase Flow* 21, 545-560 (1995)
[9] Park, S.W., Kim, S. and Lee, C.S. *Energy and Fuels* 20, 1709-1715 (2006)
[10] Wu, P.K. and Faeth, G.M. *Atomization and Sprays* 3:265-289 (1993)
[11] Gokalp, I., Chauveau, C., Simon, O. and Chesneau X. *Combustion and Flame* 89, 286-298 (1992)
[12] Kolmogorov, A.N. *Dokl. Akad. Nauk SSSR* 66:825-828 (1949)
[13] Sevik, M. and Park, S.H. *Journal of Fluids Engineering* 95,53-60 (1973)
[14] Lasheras, J.C., Villermaux, E. and Hopfinger, E.J. *Journal of Fluid Mechanics* 357,351-379 (1998)
[15] O'Loughlin W. and Masri, A.R. *Combustion and Flame* 158,1577-1590 (2011)
[16] Hardalupas, Y., Taylor, A.M.K.P. and Whitelaw, J.H. *Proceedings of the Royal Society of London. Series A, Mathematical and Physical Sciences* 426, 31-78 (1989)
[17] Chen, Y.C., Starner, S.H. and Masri, A.R. *International Journal of Multiphase Flow* 32, 389-412 (2006)
[18] Starner, S.H., Gounder, J. and Masri A.R. *Combustion and Flame* 143,420-432 (2005)